PCCP

Kinetic Monte Carlo simulations of transport diffusivities of binary mixtures in zeolites

D. Paschek and R. Krishna*

Department of Chemical Engineering, University of Amsterdam, Nieuwe Achtergracht 166, 1018 WV Amsterdam, The Netherlands. E-mail: krishna@its.chem.uva.nl; Fax: +31 20 5255604

Received 2nd March 2001, Accepted 8th June 2001
First published as an Advance Article on the web 6th July 2001

We develop the Maxwell–Stefan formulation for diffusion of binary mixtures in zeolites, and show that the mixture transport behaviour can be predicted on the basis of information on the pure component jump diffusivities at zero loading. The interaction between the diffusing, sorbed, species is taken into account by the introduction of an interchange coefficient $Đ_{ij}$, which is estimated using a logarithmic interpolation formula. To verify the developed Maxwell–Stefan formulation, we have carried out kinetic Monte Carlo (KMC) simulations to calculate the transport diffusivities for binary mixtures in silicalite and also on a square lattice. The KMC simulations confirm that the binary mixture diffusion can be predicted with very good accuracy. The interchange coefficient $Đ_{ij}$ encapsulates the correlations in the molecular jumps.

1. Introduction

Zeolites are widely used as adsorbents or catalysts in separation and reaction processes.[1–3] In the design of zeolite based processes, it is essential to have a proper description of diffusion of mixtures within the zeolite crystals. The estimation of the mixture diffusion within zeolites is complicated by several factors: (1) diffusion is closely linked with the sorption strength and is strongly influenced by the molecular loading or occupancy; (2) each of the diffusing species influences the other, the molecule with the higher mobility being retarded and the species with the lower mobility being accelerated and (3) the activated jumps of molecules are correlated because the total number of sites within the zeolite matrix is fixed, such correlation effects depending on the molecular loading and zeolite topology.

Transport of mixtures is described by a square matrix of Fick diffusivities $[D]$ for which the non-diagonal elements have significant non-zero values.[1,4] The elements of the matrix $[D]$ are influenced not only by the species mobilities but also by the sorption thermodynamics.[4] For design purposes it is important to have a mixture diffusion theory with the capability of predicting the elements of $[D]$ from pure component transport data. Such mixture diffusion theories are almost invariably based on the theory of irreversible thermodynamics (IT) and correctly recognise that chemical potential gradients must be used as the proper driving forces for diffusion.[1,4–8] This IT approach, when applied to a binary mixture, shows that the mixture diffusion is described by a square matrix of Onsager coefficients $[L]$ in which the diagonal elements are non-zero. When the matrix $[L]$ is "corrected" to take account of sorption thermodynamic effects, we obtain the Fick matrix $[D]$. The estimation of $[D]$ is therefore a matter of estimating the Onsager matrix $[L]$, but, unfortunately, the IT theory provides no fundamental guidelines for estimating $[L]$. Sundaram and Yang[8] give some estimation methods for $[L]$ but their approach is flawed, as we will demonstrate in this paper. The alternative Maxwell–Stefan (MS) approach to mixture diffusion has several advantages over the Onsager formulation. The MS approach promises to provide a convenient method for predicting the mixture transport behaviour using information on pure component transport properties, along with mixture sorption thermodynamics. Though the MS theory appears to be well developed,[4–6] its predictive capabilities have never been thoroughly tested. For verification of the mixture diffusion theories we need experimental and molecular simulation data for a wide range of mixture compositions and loadings.

While there are several experimental, and computational, studies on single species diffusion,[1,2] there is very little corresponding data on mixture diffusion. Snurr and Kärger[9] performed pulsed field gradient (PFG) NMR measurements and molecular dynamics (MD) simulations on *self diffusivities* in a mixture of CH_4 and CF_4 in silicalite. Jost *et al.*[10] performed similar studies for mixtures of CH_4 and xenon in silicalite. Gergidis *et al.*[11,12] studied the *self diffusivities* in a mixture of CH_4 and n-butane in silicalite using molecular dynamics and quasi-elastic neutron scattering (QENS). Paschek and Krishna[13] used kinetic Monte Carlo (KMC) simulations to study *self diffusivities* in a mixture of CH_4 and CF_4 in silicalite. In equipment design, the *transport* diffusivities $[D]$ rather than *self* diffusivities are required. We are aware of only one study that presents data on the elements of the Onsager matrix $[L]$ for binary mixtures; this is the recent paper of Sanborn and Snurr,[14] in which MD simulations are presented for mixtures of CF_4 and n-alkanes in faujasite.

In view of the heavy computational expense of MD simulations to study mixture diffusion, we resort to kinetic Monte Carlo (KMC) simulations to calculate *transport* diffusivities $[L]$ and $[D]$ in binary mixtures for a wide range of loadings and mixture compositions. Two types of topologies have been studied: silicalite and a primitive square lattice. The KMC simulations are used to test the MS theory. We begin with a brief summary of the MS theory for mixture diffusion.

2. The Maxwell–Stefan theory of diffusion in zeolites

In the Onsager IT formulation for diffusion of a mixture of n species within a zeolite matrix, a linear relation is postulated

between the fluxes and the chemical potential gradients:[1,4,7,8,14]

$$(N) = -\rho[\Theta_{sat}][L]\frac{1}{RT}\nabla(\mu) \quad (1)$$

where we use n-dimensional matrix notation. In eqn. (1) (N) represents the column matrix of molecular fluxes, N_i, expressed in molecules per square metre per second; ρ is the zeolite matrix density expressed as unit cells per m^3; Θ_i represents the loading expressed in molecules of sorbate per unit cell; $[\Theta_{sat}]$ is a diagonal matrix with elements $\Theta_{i,sat}$, representing the saturation loading of species i; R is the gas constant; T is the temperature; $\nabla(\mu)$ is the column matrix of chemical potential gradients, $\nabla\mu_i$, which represent the correct driving forces for diffusion; and $[L]$ is the square matrix of Onsager coefficients having the units $m^2\ s^{-1}$. Our definition of the Onsager coefficients differs from the usual ones in the literature (*e.g.* refs. 8, 14) by a factor $1/RT$. The Onsager matrix $[L]$ is non-diagonal, in general, and the cross-coefficients portray the coupling between species diffusion. The Onsager reciprocal relations demand that the matrix $[L]$ be symmetric, *i.e.*

$$L_{ij} = L_{ji}, \qquad i = 1, 2, \ldots, n$$

As we will demonstrate later, the Onsager IT formulation is not the most convenient one for mixtures because there is no simple procedure for estimating the elements of L_{ij}. A much more useful approach, entirely consistent with the theory of IT, is to adopt the Maxwell–Stefan (MS) formulation in which the chemical potential gradients are written as linear functions of the fluxes:[4–6]

$$-\rho\frac{\theta_i}{RT}\nabla\mu_i = \sum_{\substack{j=1\\ j\neq i}}^{n}\frac{\Theta_j N_i - \Theta_i N_j}{\Theta_{i,sat}\Theta_{j,sat}Đ_{ij}} + \frac{N_i}{\Theta_{i,sat}Đ_i}, \qquad i = 1, 2, \ldots, n \quad (2)$$

We have to reckon in general with two types of Maxwell–Stefan diffusivities: $Đ_i$ and $Đ_{ij}$. The $Đ_i$ are the diffusivities that reflect interactions between species i and the zeolite matrix; they are also referred to as jump or "corrected" diffusivities in the literature.[3] Mechanistically, the Maxwell–Stefan diffusivity $Đ_i$ may be related to the displacement of the adsorbed molecular species, ℓ, and the jump frequency, or transition probability, ν, which in general can be expected to be dependent on the total occupancy.[15,16] For a square lattice [see Fig. 1(a)], the zero-loading diffusivity can be estimated from

$$Đ_i(0) = \tfrac{1}{4}\nu\ell^2 \quad (3)$$

where the jump probabilities in the x and y directions are taken to be identical. For a cubic lattice [see Fig. 1(b)] we obtain

$$Đ_i(0) = \tfrac{1}{6}\nu\ell^2 \quad (4)$$

For the silicalite topology [see Fig. 1(c)], Kärger[17] has derived the following set of relations:

$$Đ_i(0) = \tfrac{1}{3}[Đ_x(0) + Đ_y(0) + Đ_z(0)]; \qquad Đ_x(0) = \tfrac{1}{4}\nu_{zz}a^2;$$

$$Đ_y(0) = \tfrac{1}{4}\nu_{str}b^2; \qquad Đ_z(0) = \frac{1}{4}\frac{\nu_{str}\nu_{zz}}{\nu_{zz}+\nu_{zz}}c^2 \quad (5)$$

where ν_{str} and ν_{zz} are the jump frequencies for movement along the straight (str) and zig-zag (zz) channels respectively and the dimensions a, b and c are as specified in Fig. 1. The Kärger formula given by eqn. (5) is however restricted in its applicability to molecules which are predominantly located at the intersections. For specific molecules, the zero-loading diffusivity $Đ_i(0)$ can be determined experimentally or by use of transition state theory.[18–22]

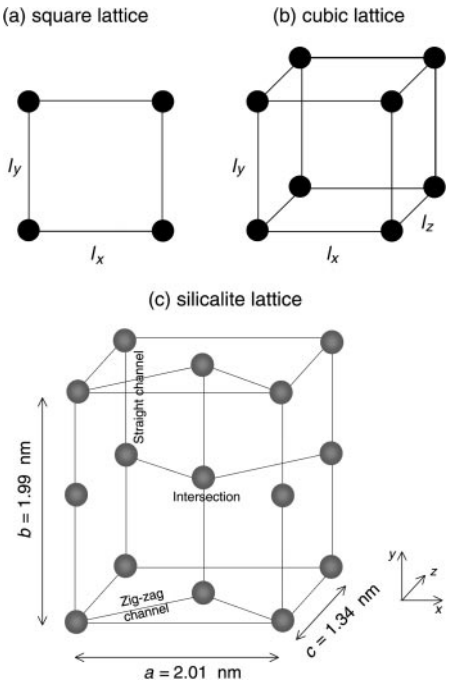

Fig. 1 Diffusion unit cells for (a) square lattice, (b) cubic lattice and (c) silicalite. The large dots indicate the sorption sites. For silicalite we consider a maximum of four sorption sites per unit cell, located at the intersections between the straight and zig-zag channels.

The jump frequency ν can be expected to decrease with occupancy.[15,16,23] If we assume that a molecule can migrate from one site to another only when the receiving site is vacant, the chance that this will occur will be a function of the fraction of unoccupied sites. The loading dependence of the jump diffusivity is therefore $Đ_i = Đ_i(0) \times$ (vacancy factor), where $Đ_i(0)$ represents the Maxwell–Stefan diffusivity in the limit of zero loading. The vacancy factor can be taken to be $(1 - \theta_1 - \theta_2 - \cdots - \theta_n)$ and therefore we get

$$Đ_i = Đ_i(0)(1 - \theta_1 - \theta_2 - \cdots - \theta_n) \quad (6)$$

Additionally, molecular repulsive forces come into play when determining the jump frequency of molecules. Due to molecular repulsions the jump frequency increases because a molecule wishes to escape from the "unfavourable" environment. Clearly, the molecular repulsions will increase when the occupancy increases. If the repulsion factor is proportional to $1/(1 - \theta_1 - \theta_2 - \cdots - \theta_n)$, we see that the Maxwell–Stefan diffusivity is independent of the molecular loading. There is a considerable amount of experimental data to show that the Maxwell–Stefan diffusivity $Đ$ is indeed independent of the loading.[1–3] In the KMC simulations to be described later we did not introduce molecule–molecule repulsions; for this scenario we would expect eqn. (6) to hold, *i.e.* the Maxwell–Stefan diffusivity decreasing with increasing loading due to reduced vacancies.

Mixture diffusion introduces an additional complication due to sorbate–sorbate interactions. This interaction is embodied in the coefficients $Đ_{ij}$. We can consider this coefficient as representing the facility for counter-exchange, *i.e.* at a sorption site the sorbed species j is replaced by the species i. Fig. 2 is a pictorial representation of the exchange process. The Onsager reciprocal relations require $Đ_{ij} = Đ_{ji}$. The net effect of this counter-exchange is a slowing down of a faster moving species due to interactions with a species of lower mobility. Also, a species of lower mobility is accelerated by interactions with another species of higher mobility. We will see later that $Đ_{ij}$ encapsulates the correlation effects associated with molecular jumps. The interchange coefficient $Đ_{ij}$ can be

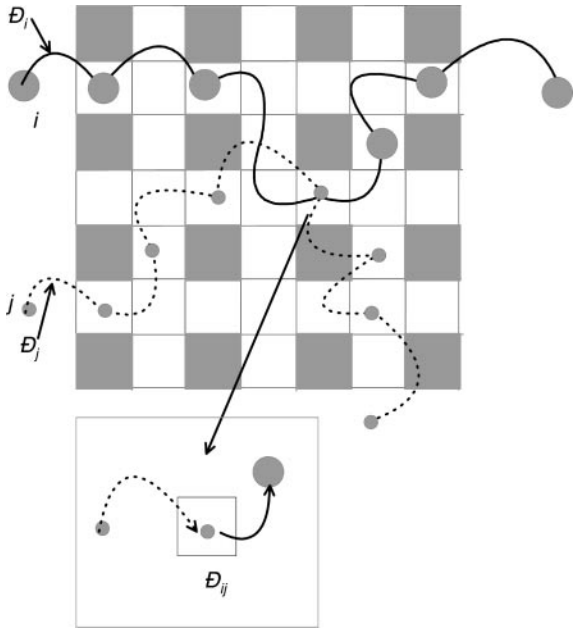

Fig. 2 Pictorial representation of the two types of diffusivities for binary mixtures using the Maxwell–Stefan model.

estimated by a procedure that has been suggested by Krishna and Wesselingh:[4]

$$Đ_{ij} = [Đ_i]^{\theta_i/(\theta_i+\theta_j)}[Đ_j]^{\theta_j/(\theta_i+\theta_j)} \tag{7}$$

It is convenient to introduce the matrix of thermodynamic factors $[\Gamma]$, defined by

$$\Gamma_{ij} \equiv \left(\frac{\Theta_{j,\,\mathrm{sat}}}{\Theta_{i,\,\mathrm{sat}}}\right)\frac{\Theta_i}{p_i}\frac{\partial p_i}{\partial \Theta_j} = \theta_i \frac{\partial \ln p_i}{\partial \theta_j}, \qquad i, j = 1, 2, \ldots, n \tag{8}$$

where p_i represent the partial pressures of the components in the vapour phase and the θ_i represent the fractional occupancies of the species:

$$\theta_i \equiv \Theta_i/\Theta_{i,\,\mathrm{sat}}, \qquad i = 1, 2, \ldots, n \tag{9}$$

Combining eqns. (1), (8) and (9) we obtain

$$(N) = -\rho[\Theta_{\mathrm{sat}}][L]\begin{bmatrix} 1/\theta_1 & 0 & 0 \\ 0 & \ddots & 0 \\ 0 & 0 & 1/\theta_n \end{bmatrix}[\Gamma](\nabla\theta) \tag{10}$$

Also, eqn. (2) can be cast into n-dimensional matrix form:

$$(N) = -\rho[\Theta_{\mathrm{sat}}][B]^{-1}[\Gamma]\nabla(\theta) \tag{11}$$

The matrix $[B]$ has the elements

$$B_{ii} = \frac{1}{Đ_i} + \sum_{\substack{j=1 \\ j\neq i}}^{n}\frac{\theta_j}{Đ_{ij}}, \qquad B_{ij} = -\frac{\theta_i}{Đ_{ij}}, \qquad i, j = 1, 2, \ldots, n \tag{12}$$

If the square matrix of Fick, or transport, diffusivities, $[D]$, is defined by

$$(N) = -\rho[\Theta_{\mathrm{sat}}][D](\nabla\theta) \tag{13}$$

we obtain the following inter-relations and a method for estimation the elements of $[D]$:

$$[D] = [L]\begin{bmatrix} 1/\theta_1 & 0 & 0 \\ 0 & \ddots & 0 \\ 0 & 0 & 1/\theta_n \end{bmatrix}[\Gamma] = [B]^{-1}[\Gamma] \tag{14}$$

If the n-component sorption can be described by the multicomponent Langmuir isotherm, the elements of $[\Gamma]$ are given by

$$\Gamma_{ij} = \delta_{ij} + \frac{\theta_i}{1-\theta_1-\theta_2-\cdots-\theta_n}, \qquad i, j = 1, 2, \ldots, n \tag{15}$$

where δ_{ij} is the Kronecker delta.

Even though the Onsager and MS formulations are formally equivalent, the important advantage of the MS formulation is that eqns. (3)–(9) allow calculation of the matrices $[D]$ and $[L]$ for multicomponent mixtures from data on pure components.

The above derivation was for a general n-component mixture. Let us examine two important limiting cases of the general formalism: (a) pure component diffusion and (b) tracer diffusion.

For diffusion of a single species obeying the Langmuir sorption isotherm we obtain:

$$N_1 = -\rho\Theta_{1,\,\mathrm{sat}}D_1\nabla\theta_1 = -\rho\Theta_{1,\,\mathrm{sat}}Đ_1\frac{1}{1-\theta_1}\nabla\theta_1$$

$$= -\rho\Theta_{\mathrm{sat}}L_1\frac{1}{\theta_1}\frac{1}{1-\theta_1}\nabla\theta_1 \tag{16}$$

where D_1, $Đ_1$ and L_1 are respectively the Fick, MS and Onsager coefficients; these are inter-related as

$$L_1 = Đ_1\theta_1 = D_1(1-\theta_1)\theta_1 \tag{17}$$

Let us apply the above set of equations for self diffusion and consider a system consisting of untagged (1) and tagged (2) species. For self diffusion the conditions of the experiment are such that the gradients for diffusion of the tagged and untagged species are equal in magnitude and opposite in sign:

$$\nabla\theta_1 + \nabla\theta_2 = 0 \tag{18}$$

Consequently the fluxes of tagged and untagged species sum to zero:

$$N_1 + N_2 = 0 \tag{19}$$

Applying the restrictions (18) and (19) to eqn. (2) we obtain, after imposing $Đ_1 = Đ_2$ for the tagged and untagged species:

$$N_1 = -\rho\Theta_{1,\,\mathrm{sat}}D_1^*\nabla\theta_1$$

$$= -\rho\Theta_{1,\,\mathrm{sat}}\frac{1}{(1/Đ_1) + (\theta_1+\theta_2)/Đ_{12}}\nabla\theta_1 \tag{20}$$

which shows that the tracer diffusivity D_1^* is

$$D_1^* = \frac{1}{(1/Đ_1) + (\theta/Đ_{12})} \tag{21}$$

where θ is the total occupancy (tagged and untagged species). The exchange parameter $Đ_{12}$ is an expression of the *correlation* between the jumps of the tagged and untagged species. Eqn. (21) shows that the tracer, or self, diffusivity D_1^* reduces to the Maxwell–Stefan diffusivity only when the interchange coefficient is exceedingly high:

$$D_1^* \to Đ_1 \quad \text{when} \quad Đ_{12} \to \infty \tag{22}$$

In the more general case for finite values of the exchange parameter $Đ_{12}$ we would expect D_1^* to be smaller than $Đ_1$. We should in general anticipate that the interchange coefficient is related in some way to the mobility of the species 1. We may therefore assume

$$Đ_{12} = Đ_1 \tag{23}$$

and therefore the expression for the self diffusivity reduces to

$$D_1^* = \frac{Đ_1}{(1+\theta)} \tag{24}$$

If we follow the Onsager formulation (1) we can analogously derive the following expression for the self diffusivity:

$$\boldsymbol{N}_1 = -\rho\Theta_{\text{sat}} L_1^{*}\nabla\theta_1 = -\rho\Theta_{\text{sat}}\left(\frac{L_{11}}{\theta_1} - \frac{L_{12}}{\theta_2}\right)\nabla\theta_1 \qquad (25)$$

Eqn. (25) was first derived by Kärger.[7] It is important to emphasise that the coefficient L_{11} on the right hand side of eqn. (25) cannot be identified with the pure component Onsager coefficient L_1; we return to this point later on in this paper.

In order to test the capability of the MS formulation to predict mixture transport from pure component diffusivities, we resort to KMC simulations.

3. Kinetic Monte Carlo simulation methodology

We first perform kinetic Monte Carlo (KMC) simulations in which each component follows Langmuir isotherm behaviour. We assume the lattice to be made up of equal sized sites which can be occupied by only one molecule at a time. Particles can move from one site to a neighbouring site *via* hops. Two types of topologies were studied: (a) square lattice and (b) silicalite; see Fig. 1. For the square lattice [Fig. 1(a)] we take the distance of separation between adjacent sites to be unity, $\ell = 1$. Furthermore the jump frequency of species 1 is taken to be equal in all directions and set to unity, *i.e.*, $\nu_1 = 1$. For simulations with silicalite, the jump frequencies along the straight and zig-zag channels for component 1 are taken to correspond to that for 2-methylhexane (2MH) at 300 K, $\nu_{1,\text{str}} = 1.4 \times 10^5$ s^{-1}, $\nu_{1,zz} = 5 \times 10^4$ s^{-1}; these values were calculated by Smit *et al.* using the transition state theory.[19] For the silicalite topology the maximum loading was taken to be four molecules per unit cell, where the molecules are all located at the intersections. We have published the details of the pure component 2MH simulations earlier.[24] In the two-component mixture simulations, the corresponding jump frequencies for component 2 were chosen such that ν_2/ν_1 varied between 1 and 16. This allowed insight to be gained into transport in mixtures with differing mobilities.

We employ a standard KMC methodology to propagate the system (details in refs. 24–27). A hop is made every KMC step and the system clock is updated with variable time steps. For a given configuration of random walkers on the lattice a process list containing all possible M moves to vacant intersection sites is created. Each possible move i is associated with a transition probability ν_i. Now, the mean elapsed time τ is the inverse of the total rate coefficient

$$\tau^{-1} = \nu_{\text{total}} = \sum_{i=1}^{M} \nu_i \qquad (26)$$

which is then determined as the sum over all processes contained in the process list. The actual KMC time step Δt for a given configuration is randomly chosen from a Poisson distribution

$$\Delta t = -\ln(u)/\nu_{\text{total}} \qquad (27)$$

where $u \in [0,1]$ is a uniform random deviate. The time step Δt is independent of the chosen hopping process. To select the actual jump, we define process probabilities according to

$$p_i = \sum_{j=1}^{i} \nu_j/\nu_{\text{total}}$$

The ith process is chosen, when $p_{i-1} < \nu < p_i$, where $\nu \in [0,1]$ is another uniform random deviate. After having performed a hop, the process list is updated. In order to avoid wall effects we employ periodic boundary conditions. We have investigated the finite size effect on the diffusivity and found systems of 10×10 and $6 \times 6 \times 6$ unit cells to be sufficiently large for the 2D and 3D lattices shown in Fig. 1. In order to provide sufficiently accurate data for the Onsager transport coefficient L_{ij}, a total of 10^8 to 10^9 simulation steps were required.These simulations extended to several CPU days on a single IBM SP2 node.

For diffusion of a single component 1, the details of the determination of the self diffusivity D_1^{*}, the jump diffusivity $Đ_1$ and the transport diffusivity D_1 from the ensemble average statistics have been published earlier.[24] For binary mixtures, applying linear response theory, the Onsager coefficients L_{ij} can be determined using the displacement formula

$$\begin{aligned} L_{ij} &= \lim_{\Delta t\to\infty} L_{ij}(\Delta t) \\ &= \frac{1}{6}\frac{1}{N_s}\lim_{\Delta t\to\infty}\frac{1}{\Delta t}\left\langle\left(\sum_{l=1}^{N_i}[\boldsymbol{r}_{l,i}(t+\Delta t) - \boldsymbol{r}_{l,i}(t)]\right)\right. \\ &\quad \left.\times\left(\sum_{k=1}^{N_j}[\boldsymbol{r}_{k,j}(t+\Delta t) - \boldsymbol{r}_{k,j}(t)]\right)\right\rangle \end{aligned} \qquad (28)$$

where $\langle\cdots\rangle$ denotes both ensemble and time averaging over the entire system trajectory; N_i is the number of particles belonging to species i; and $\boldsymbol{r}_i(t)$ is the position vector of component i at time t. In contrast to the formula for L_{ij} used by Sanborn and Snurr[14] in their MD simulations, the normalising volume is replaced by N_s, the total number of discrete adsorption sites in the simulation. For the square lattice simulations, we use a pre-multiplier 1/4 instead of 1/6 in eqn. (6). Furthermore, eqn. (28) yields L_{ij} in units of m^2 s^{-1}. The Onsager coefficients L_{ij} are subject to strong correlation effects and therefore the obtained values of the transport coefficients vary strongly with the separation time between two configurations Δt. This is illustrated in Fig. 3 for binary mixture simulations for the square lattice configuration for which $\nu_2/\nu_1 = 16$. Since arbitrary time and length units have been used for the square lattice simulations, the Onsager coefficients presented in Fig. 3, and also later in this paper, have been normalised with respect to the zero-loading diffusivity of component 1, $Đ_1(0)$. We see from Fig. 3 that it is important to employ a sufficiently large Δt to ensure converged data. For the square lattice simulations a Δt of 30 time steps was chosen. For simulations with silicalite, using actual lattice dimensions and realistic jump frequencies, a Δt of 10^{-3} s was employed, on the basis of our previous experience.[24,25]

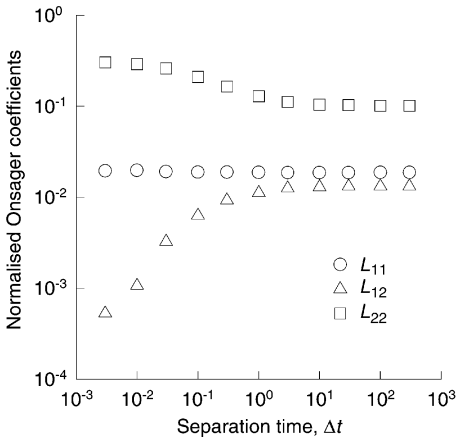

Fig. 3 The Onsager transport coefficients L_{ij} as a function of the separation time Δt for a square lattice ($\ell_x = \ell_y = 1$) with particle jump probabilities $\nu_1 = 1$, $\nu_2 = 16$, at a total occupancy $\theta = 0.96$ and a mixture composition $x_1 = x_2 = 0.5$. All the Onsager coefficients have been normalised with respect to the zero loading of component 1, $Đ_1(0)$.

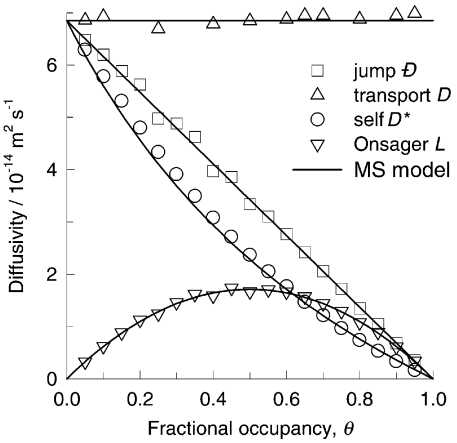

Fig. 4 KMC simulations of jump, transport, Onsager and self diffusivities of 2MH in silicalite at 300 K. The continuous lines represent the calculations using eqns. (6), (17) and (24).

4. KMC simulation results compared to the MS model predictions

Let us first consider the KMC simulation results for pure component 2MH in silicalite at 300 K. The simulations for the self diffusivity D_1^*, the jump diffusivity $Đ_1$ and the transport diffusivity D_1 for various fractional occupancies are shown in Fig. 4. The pure component Onsager coefficient L_1 calculated using eqn. (17) is also shown here. The jump diffusivity $Đ_1$ shows a linear dependence on the fractional vacancy, in conformity with eqn. (6), and the transport D_1 is seen to be independent of occupancy. Both the jump and transport diffusivities are free of correlation effects; see our earlier publication[24] for detailed discussion on this. The self diffusivity D_1^* values from KMC simulations compare very well with the estimations from eqn. (24); D_1^* is strongly influenced by correlated jump effects, evidenced by the deviation from the $(1-\theta)$ linear dependence exhibited by $Đ_1$.

Now, let us consider transport in a mixture of 2MH along with another component 2. First we take the component 2 to have identical jump frequencies along the straight and zig-zag channels as those for component 1. The simulated L_{ij} values using eqn. (28) are shown in Fig. 5 for three types of simulations: (a) 50–50 mixture with varying fractional occupancy, (b) for a total occupancy of 0.48 with varying composition of x_1, and (c) for a total occupancy of 0.96 with varying composition of x_1. Let us first consider Fig. 5(a). We note that the cross-coefficient L_{12} is non-zero despite the fact that component 2 is taken to be identical to component 1 with respect to its particle mobility. For the 50–50 mixture, $L_{11} = L_{22}$, as expected, but it is remarkable to note that these values are significantly lower than the pure component Onsager coefficient L_1 [these values of L_1 were taken from the simulations shown in Fig. 4; the values are re-plotted in Fig. 5(a) for comparison purposes]. This underlines the lack of predictability of the Onsager coefficients from pure component diffusivities. The results shown in Fig. 5(a) refute the assumption of Sundaram and Yang[8] that the diagonal elements of $[L]$ can be identified with the pure component L_i values.

Also shown in Fig. 5(a) are the estimations of the L_{ij} using eqns. (6), (7), (12) and (14), derived from the MS formulations. The agreement with the KMC simulations is excellent. Comparison of the KMC simulations with varying mixture compositions for $\theta = 0.48$ and 0.96, shown in Figs. 5(b) and (c)

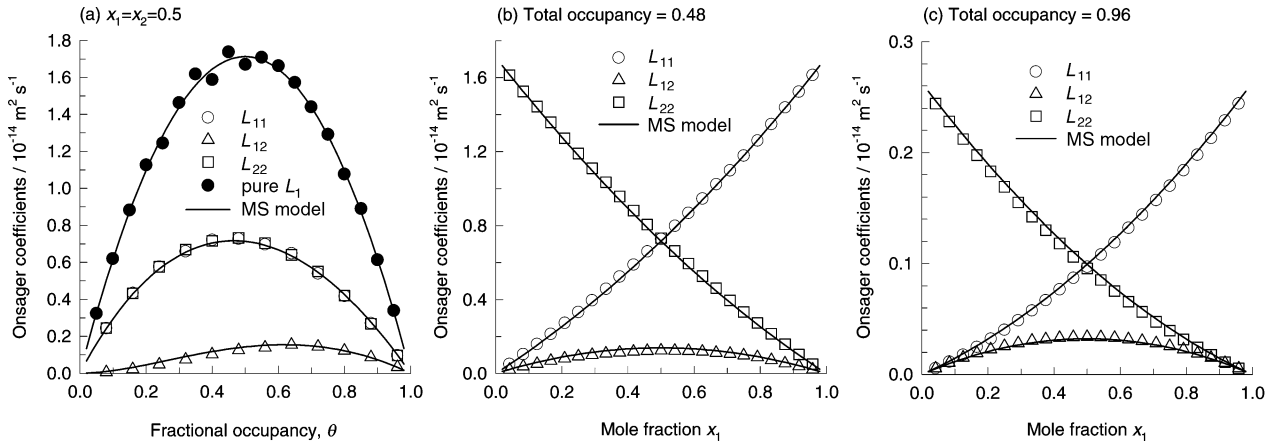

Fig. 5 KMC simulations of the Onsager coefficients L_{ij} for a binary mixture of component 1 (taken to be 2MH) and 2 in silicalite at 300 K. The jump frequencies of both components are taken to be identical to each other, $v_{str} = 1.4 \times 10^5\ s^{-1}$, $v_{zz} = 5 \times 10^4\ s^{-1}$.

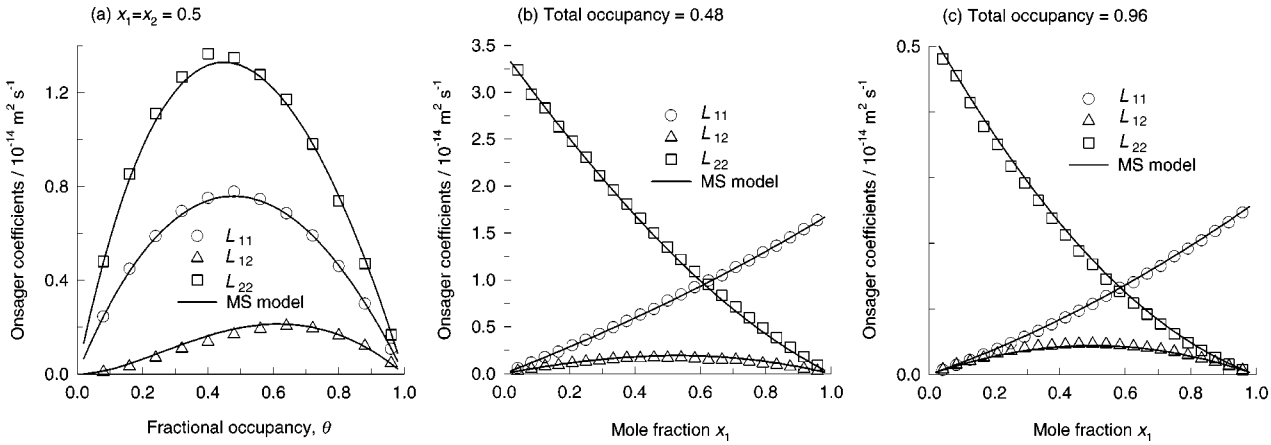

Fig. 6 KMC simulations of the Onsager coefficients L_{ij} for a binary mixture of components 1 (taken to be 2MH) and 2 in silicalite at 300 K. The jump frequencies of component 2 are taken to be twice those of component 1, *i.e.* $v_{2,str} = 2.8 \times 10^5\ s^{-1}$, $v_{2,zz} = 1 \times 10^5\ s^{-1}$.

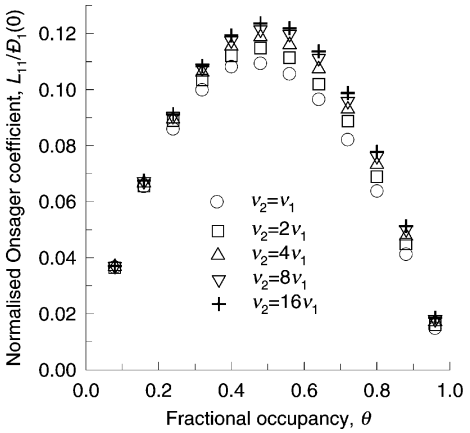

Fig. 7 KMC simulations of the Onsager coefficient L_{11} for a binary mixture in a square lattice. The lattice parameters are $\ell = 1$ and the jump frequency of component 1 is $v_1 = 1$. The ratio v_2/v_1 is varied progressively from 1 to 16. The Onsager coefficient has been normalised with respect to the zero-loading diffusivity value $Đ_1(0)$.

with the predictions of the MS theory led us to conclude that the mixture rule for the interchange coefficient, eqn. (7), is the correct one.

In Fig. 6, KMC simulation results are presented for the case in which the jump probabilities for component 2 are taken to be twice the corresponding values for component 1. We again note the excellent agreement between the simulated L_{ij} values with the predictions of the MS model for a wide variation in the loading and mixture composition.

Comparison of the values of L_{11} in Figs. 5 and 6 led us to conclude that this coefficient is influenced by the mobility of component 2. Specifically the values of L_{11} are higher in the mixture where the mobility of species 2 is higher, in Fig. 6. Put another way, correlated jump effects influence not only the cross-coefficient L_{12} but also the diagonal coefficients L_{11} and L_{22}. To emphasise this further, we present KMC simulations for a 50–50 mixture in a square lattice, where the mobility of component 2 is progressively increased; see Fig. 7. We note that L_{11} increases progressively with increasing mobility of component 2. The excellent predictive capabilities of the MS model to describe the variation of the transport coefficients with mixture composition are demonstrated in Fig. 8, which presents the KMC simulation results (square lattice, $v_2/v_1 = 16$, total occupancy = 0.96) for L_{ij}. The agreement of the MS model, using eqns. (6), (7), (12) and (14), with the KMC simulations is excellent.

Finally, we study the influence of topology on the Onsager coefficients, after normalisation by dividing by $Đ_1(0)$, by comparing the results for the silicalite topology with the corresponding results for the square lattice; the KMC results for $v_2/v_1 = 2$ are compared in Fig. 9. Interestingly, we note that the normalised transport coefficients for these two topologies are remarkably close to one another.

Eqns. (14) and (15) allow the calculation of the elements of the Fick matrix $[D]$ from information of the Onsager matrix $[L]$. From the KMC simulated $[L]$ for a square lattice with $v_1 = 1$, $v_2/v_1 = 16$, we have calculated the elements of $[D]$ for a variety of loadings and mixture compositions; these are shown in Fig. 10 along the predictions of the MS theory from pure component transport data. The agreement can be considered to be very good. Examination of the elements of $[D]$ shows that the non-diagonal elements D_{12} and D_{21} increase

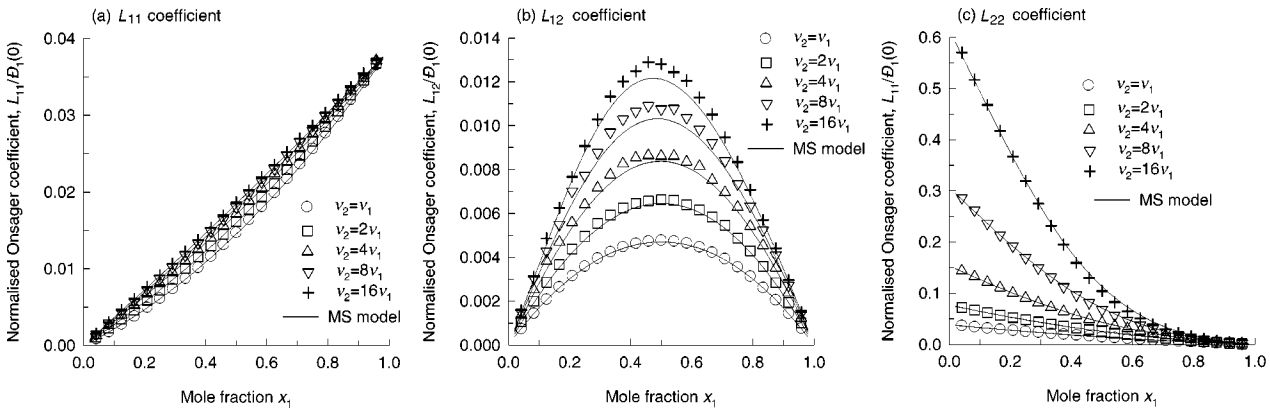

Fig. 8 KMC simulations of the Onsager coefficient L_{ij} for a binary mixture, of varying composition x_1, in a square lattice. The total occupancy of the lattice is 0.96. The lattice parameters are $\ell = 1$ and the jump frequency of component 1 is $v_1 = 1$. The ratio v_2/v_1 is varied progressively from 1 to 16. The Onsager coefficient has been normalised with respect to the zero-loading diffusivity value $Đ_1(0)$. The symbols are the KMC simulations and the continuous lines represent the calculations of the Maxwell–Stefan model.

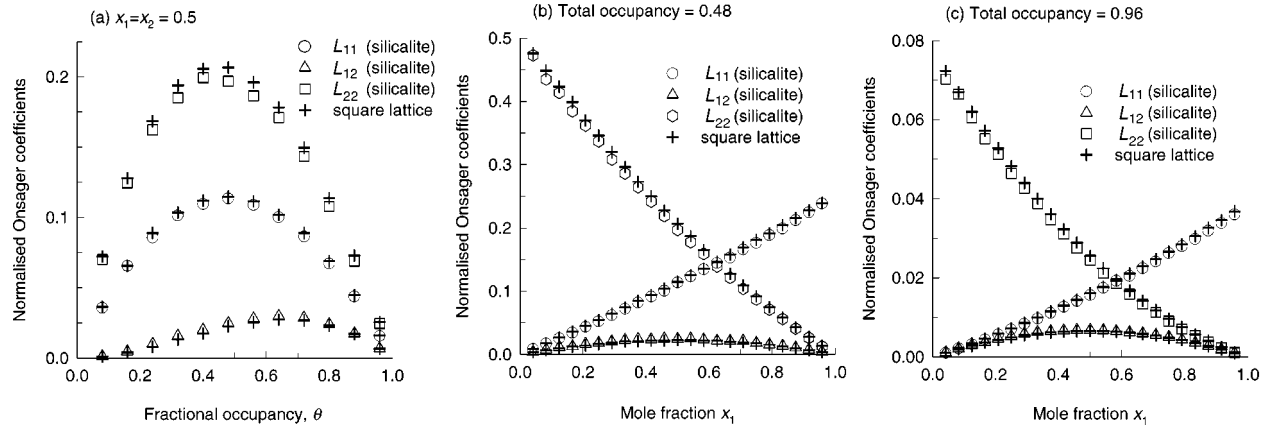

Fig. 9 KMC simulations of the normalised Onsager coefficients L_{ij} for a binary mixture of components 1 (taken to be 2MH) and 2 in silicalite at 300 K compared with the corresponding results obtained for a square lattice ($v_1 = 1$, $v_2/v_1 = 2$). The Onsager coefficient has been normalised with respect to the zero-loading diffusivity value $Đ_1(0)$.

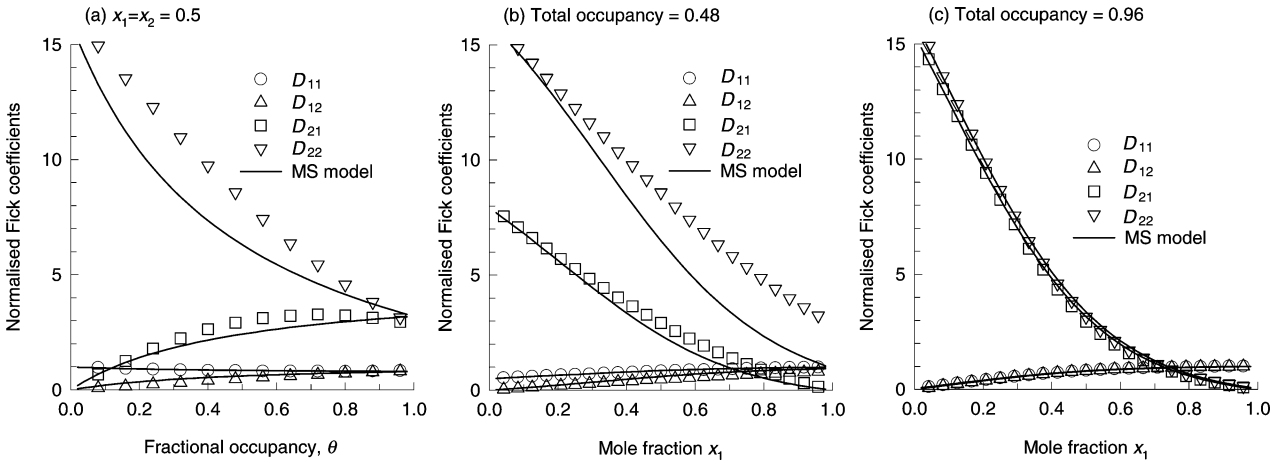

Fig. 10 KMC simulations of the normalised Fick coefficients D_{ij} for a binary mixture of components 1 and 2 in a square lattice ($v_1 = 1$, $v_2/v_1 = 16$). The Fick coefficient has been normalised with respect to the zero-loading diffusivity value $Đ_1(10)$ The symbols are the KMC simulations and the continuous lines represent the calculations of the Maxwell–Stefan model.

with increasing total occupancy and can attain values comparable to the main coefficients D_{11} and D_{22}; this shows that, in mixture diffusion, the flux of one species is very strongly coupled to that of the other species.

5. Conclusions

We have developed the MS formulation for mixture diffusion in zeolites and compared this with the Onsager formulation. Both approaches have their roots in the theory of irreversible thermodynamics. An important advantage of the MS formalism is that it allows the estimation of mixture diffusion on the basis of the pure component diffusivities at zero loading. This predictive capability has been tested by carrying out KMC simulations in both silicalite and a primitive square lattice. The following major conclusions can be drawn from the results presented in this paper.

(i) For single component diffusion, the self diffusivity is subject to correlation effects (*cf.* Fig. 4); these correlation effects are captured by the interchange coefficient $Đ_{12}$. A good approximation is to take $Đ_{12}$ to be equal to the pure component jump diffusivity $Đ_1$; this assumption is verified by the results presented in Fig. 4.

(ii) For binary mixture diffusion, the diagonal element L_{11} cannot be identified with the pure component Onsager coefficient L_1; *cf.* Fig. 5(a). This erroneous assumption has been made in the zeolite literature[8] to derive mixture diffusion theories.

(iii) For binary mixture diffusion, L_{11} is influenced by the mobility of species 2; *cf.* Fig. 7. This further emphasises the fact that L_{11} cannot be identified with the pure component L_1 as has been suggested by Sundaram and Yang.[8]

(iv) All three Onsager coefficients L_{ij} are influenced by correlated jump effects. This result is in sharp contrast with the MS diffusivities $Đ_i$ which are free of correlation effects.[24]

(v) The set of KMC simulation results presented in Figs. 5, 6 and 8 validate the excellent predictive capability of the MS formulation.The logarithmic interpolation formula [eqn. (7)] for the interchange coefficient has been verified.

(vi) Comparison of the square lattice simulations with those of silicalite, for the same mobility ratios in the results presented in Fig. 9 (taking $v_2/v_1 = 2$), shows that the *normalised* transport coefficients are comparable in magnitude and show the same trend with mixture loading and composition.

(vii) From knowledge of the Onsager $[L]$ matrix, the elements of the Fick (or transport) matrix $[D]$ can be obtained using eqns. (15) and (16). The results presented in Fig. 10 underline the strong coupling effects for a mixture with widely different mobilities.

The overall conclusion of our study is that the Maxwell–Stefan formulation provides a reliable procedure for estimation of the diffusion behaviour of binary mixtures in zeolites on the basis of the information on pure component transport properties, along with mixture sorption thermodynamics.

Acknowledgements

RK and DP acknowledge a grant *Programmasubsidie* from the Netherlands Organisation for Scientific Research (NWO) for development of novel concepts in reactive separations technology.

References

1 J. Kärger and D. M. Ruthven, *Diffusion in Zeolites and Other Microporous Solids*, Wiley, New York, 1992.
2 D. M. Ruthven and M. F. M. Post, Diffusion in zeolite molecular sieves, in *Introduction to Zeolite Science and Practice*, ed. H. van Bekkum, E. M. Flanigan and J. C. Jansen, Elsevier, Amsterdam, 2nd edn., 2000.
3 D. M. Ruthven, *Principles of Adsorption and Adsorption Processes*, Wiley, New York, 1984.
4 R. Krishna and J. A. Wesselingh, *Chem. Eng. Sci.*, 1997, **52**, 861.
5 F. Kapteijn, J. A. Moulijn and R. Krishna, *Chem. Eng. Sci.*, 2000, **55**, 2923.
6 R. Krishna and D. Paschek, *Sep. Pur. Technol.*, 2000, **21**, 111.
7 J. Kärger, *Surf. Sci.*, 1973, **36**, 797.
8 N. Sundaram and R. T. Yang, *Chem. Eng. Sci.*, 2000, **55**, 1747.
9 R. Q. Snurr and J. Kärger, *J. Phys. Chem. B*, 1997, **101**, 6469.
10 S. Jost, N. K. Bär, S. Fritzsche, R. Haberlandt and J. Kärger, *J. Phys. Chem. B*, 1998, **102**, 6375.
11 L. N. Gergidis, D. N. Theodorou and H. Jobic, *J. Phys. Chem. B*, 2000, **104**, 5541.
12 L. N. Gergidis and D. N. Theodorou, *J. Phys. Chem. B*, 1999, **103**, 3380.
13 D. Paschek and R. Krishna, *Langmuir*, 2001, **17**, 247.
14 M. J. Sanborn and R. Q. Snurr, *Sep. Pur. Technol.*, 2000, **20**, 1.
15 D. A. Reed and G. Ehrlich, *Surf. Sci.*, 1981, **105**, 603.
16 D. A. Reed and G. Ehrlich, *Surf. Sci.*, 1981, **102**, 588.
17 J. Kärger, *J. Phys. Chem.*, 1991, **95**, 5558.
18 R. L. June, A. T. Bell and D. N. Theodorou, *J. Phys. Chem.*, 1991, **95**, 8866.
19 B. Smit, L. D. J. C. Loyens and G. L. M. M. Verbist, *Faraday Discuss.*, 1997, **106**, 93.
20 S. Pal and K. A. Fichthorn, *Chem. Eng. J.*, 1999, **74**, 77.
21 C. Tunca and D. M. Ford, *J. Chem. Phys.*, 1999, **111**, 2751.
22 T. J. H. Vlugt, C. Dellago and B. Smit, *J. Chem. Phys.*, 2000, **113**, 8791.
23 L. Riekert, *AIChE J.*, 1971, **17**, 446.
24 D. Paschek and R. Krishna, *Phys. Chem. Chem. Phys.*, 2000, **2**, 2389.
25 D. Paschek and R. Krishna, *Chem. Phys. Lett.*, 2001, **333**, 278.
26 S. M. Auerbach, *Int. Rev. Phys. Chem.*, 2000, **19**, 155.
27 M. O. Coppens, A. T. Bell and A. K. Chakraborty, *Chem. Eng. Sci.*, 1999, **54**, 3455.